Proteomic analysis identifies the E3 ubiquitin ligase Pdzrn3 as a regulatory target of Wnt5a-Ror signaling

Sara E. Konopelski Snavely[a] , Michael W. Susman[b], Ryan C. Kunz[c], Jia Tan[a] , Srisathya Srinivasan[a] , Michael D. Cohen[a], Kyoko Okada[a], Helen Lamb[a] , Shannon S. Choi[a], Edith P. Karuna[a] , Michael K. Scales[a] , Steven P. Gygi[c], Michael Eldon Greenberg[b,1] , and Hsin-Yi Henry Ho[a,b,1]

[a]Department of Cell Biology and Human Anatomy, School of Medicine, University of California, Davis, CA 95616; [b]Department of Neurobiology, Harvard Medical School, Boston, MA 02115; and [c]Department of Cell Biology, Harvard Medical School, Boston, MA 02115

Wnt5a-Ror signaling is a conserved pathway that regulates morphogenetic processes during vertebrate development [R. T. Moon et al., Development 119, 97–111 (1993); I. Oishi et al., Genes Cells 8, 645–654 (2003)], but its downstream signaling events remain poorly understood. Through a large-scale proteomic screen in mouse embryonic fibroblasts, we identified the E3 ubiquitin ligase Pdzrn3 as a regulatory target of the Wnt5a-Ror pathway. Upon pathway activation, Pdzrn3 is degraded in a β-catenin–independent, ubiquitin-proteasome system–dependent manner. We developed a flow cytometry-based reporter to monitor Pdzrn3 abundance and delineated a signaling cascade involving Frizzled, Dishevelled, Casein kinase 1, and Glycogen synthase kinase 3 that regulates Pdzrn3 stability. Epistatically, Pdzrn3 is regulated independently of Kif26b, another Wnt5a-Ror effector. Wnt5a-dependent degradation of Pdzrn3 requires phosphorylation of three conserved amino acids within its C-terminal LNX3H domain [M. Flynn, O. Saha, P. Young, BMC Evol. Biol. 11, 235 (2011)], which acts as a bona fide Wnt5a-responsive element. This phospho-dependent degradation is essential for Wnt5a-Ror modulation of cell migration. Collectively, this work establishes a Wnt5a-Ror cell morphogenetic cascade involving Pdzrn3 phosphorylation and degradation.

Wnt5a | Pdzrn3 | Ror1 | Ror2

Embryonic development in vertebrates is a highly stereotyped and coordinated process that depends on a handful of core signaling pathways. One major mode of signaling involves Wnt ligands, a diverse and highly conserved family of glycoproteins that signal in many spatiotemporal contexts, including tissue specification and tissue morphogenesis, in addition to tissue homeostasis in adult organisms (1–3). Thus, Wnts play unique and critical roles in both developing and adult organisms.

Traditionally, Wnt pathways have been classified as either canonical or noncanonical. Canonical Wnt signaling utilizes β-catenin as a transcriptional coactivator to regulate cell fate and proliferation, and its mechanism of action and biological functions are relatively well understood. In contrast, noncanonical Wnt signaling, which regulates tissue morphogenetic processes in a β-catenin–independent manner, remains poorly characterized (1–6). Numerous studies in a variety of model organisms have demonstrated that alterations to the expression of Wnt5a, the prototypic noncanonical Wnt ligand, can cause drastic morphogenesis defects, such as body axis truncations, shortened limbs and tails, and craniofacial malformations (7–9). These phenotypic abnormalities closely mirror those of Ror1 and Ror2 double-knockout (dKO) mice, further underscoring the growing evidence that Ror receptors mediate Wnt5a signals to orchestrate tissue morphogenetic events (10, 11).

Importantly, the phenotypic characteristics observed in Wnt5a and Ror1; Ror2 double mutants have also been observed in human Robinow syndrome patients, and several recent publications have reported that many Robinow syndrome patients possess mutations in various components of the Wnt5a-Ror signaling pathway, including WNT5A, ROR2, FRIZZLED2 (FZD2), DISHEVELLED1 (DVL1), and DISHEVELLED3 (DVL3) (12–18). Furthermore,

bulldogs and other closely related dog breeds possess a mutation in DISHEVELLED2 (DVL2) that is highly analogous to the human Robinow syndrome mutations in DVL1 and DVL3, and these breeds exhibit skeletal and craniofacial features that are reminiscent of human Robinow syndrome (19). Collectively, these recent findings strongly support the idea that Wnt5a-Ror signaling is conserved and critical to tissue morphogenesis in a variety of vertebrates. However, despite the significance of Wnt5a-Ror signaling in normal development and disease contexts, the mechanisms by which Wnt5a signals are transmitted and processed within the cell remain unclear. Progress within the field is further hampered by a lack of consensus regarding the number of noncanonical pathways, the biochemical nature of their regulation, and variability in the methods used to measure signaling (4).

To deepen our understanding of Wnt5a-Ror signaling, we have taken systematic approaches to identify downstream cellular events that occur in response to pathway activation. Previously, we genetically ablated Ror1 and Ror2 receptors in primary mouse embryonic fibroblast (MEF) cultures and used a proteomic approach to uncover downstream signaling events that are misregulated. From this analysis, we identified the atypical kinesin Kif26b as a

Significance

Wnt5a-Ror signaling is a master regulator of tissue shape, and dysfunction of the pathway contributes to congenital birth defects and cancer metastasis. The molecular underpinnings of this pathway, however, remain unclear. To identify subcellular protein changes driven by Wnt5a-Ror signaling, we conducted a large-scale proteomic screen and identified the E3 ubiquitin ligase Pdzrn3 as a downstream target. Wnt5a-Ror signaling initially induces Pdzrn3 phosphorylation, which subsequently triggers the ubiquitin-proteasome–dependent degradation of Pdzrn3. Importantly, Wnt5a-Ror signaling uses this phospho-degradation process to regulate cell migration. From these findings, we further developed a flow cytometry-based reporter to monitor Pdzrn3 abundance and delineated the signaling cascade regulating Pdzrn3 stability. Collectively, our study establishes Pdzrn3 phosphorylation and degradation as a key component of Wnt5a-Ror signaling.

www.manaraa.com

downstream component of Wnt5a-Ror signaling that is degraded upon Wnt5a-Ror pathway activation (20).

In this follow-up study, we hypothesized that the identification of additional downstream regulatory targets would augment our mechanistic understanding of Wnt5a-Ror signaling. Thus, we conducted a second large-scale proteomic screen to identify cellular proteins whose abundance and phosphorylation state are altered by acute stimulation of Wnt5a-Ror signaling. Through this approach, we identified the E3 ubiquitin ligase Pdzrn3 as a downstream target. Pdzrn3 has been implicated in noncanonical Wnt signaling previously based on its interactions with Dvl3 and shown to function as a promigratory factor in several morphogenetic contexts, including synaptic growth and maturation, vascular morphogenesis, and neuronal positioning (21–23). However, how noncanonical Wnt signaling regulates Pdzrn3 at a biochemical level still remains unknown. We discovered that Pdzrn3 is degraded by Wnt5a-Ror signaling via a mechanism independent of β-catenin but dependent on the ubiquitin-proteasome system (UPS). This regulation is mediated by a signaling cascade involving Frizzled (Fzd), Dishevelled (Dvl), Casein kinase 1 (CK1), and Glycogen synthase kinase 3 (GSK3), which is remarkably similar to the cascade that regulates Kif26b. Despite these similarities, we find that Wnt5a-induced degradation of Pdzrn3 is not dependent on Kif26b and vice versa. Furthermore, Wnt5a-dependent degradation of Pdzrn3 requires phosphorylation of three specific amino acid residues on its C-terminal LNX3H domain. Critically, the phosphorylation and degradation of Pdzrn3 serves as a mechanism through which Wnt5a-Ror signaling can regulate cell migration. Finally, we demonstrated that the LNX3H domain is required for Wnt5a-dependent degradation of not only Pdzrn3 but also its structural homolog Lnx4, suggesting that the LNX3H domain may generally function as a Wnt5a-responsive domain. Together, these findings establish the mechanisms through which the Wnt5a-Ror pathway regulates Pdzrn3 abundance to facilitate signal transduction, thus providing a platform from which a deeper mechanistic and cell morphogenetic understanding of noncanonical Wnt signaling can be attained.

Results

Large-Scale Proteomic Screen Identifies the E3 Ubiquitin Ligase Pdzrn3 as a Downstream Regulatory Target of Wnt5a-Ror Signaling.
To profile both early and late molecular events driven by Wnt5a-Ror signaling, we conducted a large-scale proteomic screen in which primary embryonic day (E) 12.5 Wnt5a KO MEFs (8, 11, 20) were acutely stimulated with purified recombinant Wnt5a (rWnt5a) for 0, 1, or 6 h, and then used quantitative tandem mass tag (TMT) mass spectrometry to globally assess changes in the abundance and phosphorylation state of cellular proteins over time (Fig. 1A; see Dataset S1 for full list) (24). Two independent replicates of Wnt5a KO MEF cultures were analyzed for rigor and reproducibility. Potential proteins of interest were defined as tryptic peptides or phospho-tryptic peptides that exhibited 1) a negative or positive change of >1.5-fold in abundance and 2) a change with a $P < 0.05$ across the two replicates.

Based on these criteria, our top candidate was Pdzrn3, an E3 ubiquitin ligase that exhibited significant changes in both steady-state protein abundance and phosphorylation state after rWnt5a stimulation. Although 1 h of rWnt5a stimulation did not yield any detectable changes, after 6 h of rWnt5a stimulation we observed that Pdzrn3 abundance was significantly down-regulated by 1.72-fold ($P = 0.013$) (Fig. 1 B, C, and F and SI Appendix, Table S1). Additionally, we identified multiple phospho-tryptic peptides derived from two different regions of Pdzrn3 that exhibited significant changes after rWnt5a stimulation (Fig. 1 D and E). A phospho-tryptic peptide containing S843 and S845 (dotted line in Fig. 1G) and another one containing T955, T956, and S962 (dashed line in Fig. 1G) both showed an initial increase at 1 h, followed by a decrease at 6 h. Similarly, a third phospho-tryptic peptide containing

S775 (dotted dashed line in Fig. 1G), though not a "hit" based on its significance value ($P = 0.076$), also exhibited a similar pattern of change. Finally, a phospho-tryptic peptide containing S845 (solid line in Fig. 1G) decreased gradually after 1 h and more extensively after 6 h. Importantly, all phospho-tryptic peptides decreased by 6 h to a similar extent as that of the nonphosphorylated tryptic peptide (Fig. 1F). This overall pattern thus raised the hypothesis that Wnt5a signaling first induces the phosphorylation of Pdzrn3 at 1 h, followed by down-regulation of Pdzrn3 protein abundance at 6 h, and these two biochemical events are kinetically and mechanistically coupled.

In addition to Pdzrn3, the proteomic screen also identified other known components of the Wnt5a-Ror signaling pathway (SI Appendix, Table S1). At both the 1-h and 6-h timepoints, a phospho-tryptic peptide from Kif26b was scored as a "hit" (1.70- and 2.03-fold decrease, respectively). At the 6-h timepoint, a phospho-tryptic peptide from CK1 isoform γ-3 was also scored as a "hit" (1.52-fold increase). Moreover, a phospho-tryptic peptide from Dvl2 exhibited a 1.49-fold increase in abundance after 6 h of rWnt5a stimulation. The identification of these previously described Wnt5a signaling targets further validates the selectivity and sensitivity of the proteomic screening approach. Other hits of interest include Irf2bpl, another E3 ubiquitin ligase, which has been shown to reduce canonical Wnt signaling in gastric cancer (25), as well as several proteins with connections to the cytoskeleton, such as Cttnbp2nl (26), Jmy (27–29), Cit (30), Svil (31, 32), Ppfibp1 (33), Marcks (34, 35), Cald1 (36–38), and Map2 (39, 40) or tisse morphogenesis, including Fam193a and Nhs1 (41, 42).

To independently confirm that Pdzrn3 abundance is indeed regulated by Wnt5a signals, we generated rabbit polyclonal antibodies against Pdzrn3 and used Western blotting to analyze the steady-state cellular levels of Pdzrn3 after rWnt5a stimulation. Consistent with our proteomic screening results, we observed that the abundance of Pdzrn3 significantly decreased after 6 h of rWnt5a stimulation (Fig. 2 A and B). This change parallels other previously described responses of Wnt5a-Ror signaling, including increased phosphorylation of Ror1, Ror2, and Dvl2, and decreased Kif26b abundance (Fig. 2 A and B) (11, 20).

To test whether Ror receptors are required for Wnt5a signaling to Pdzrn3, we utilized conditional Ror receptor family KO MEFs derived from E12.5 $Ror1^{fl/fl};Ror2^{fl/fl};CAG-CreER$ embryos. These MEFs undergo robust autocrine/paracrine Wnt5a-Ror signaling without exogenous Wnt5a (11). We treated cells with 4-hydroxytamoxifen (4OHT) to induce CreER-mediated deletion of the $Ror1^{fl/fl}$ and $Ror2^{fl/fl}$ alleles. We observed that loss of Ror receptor expression significantly increased Pdzrn3 levels, which correlated with decreased Dvl2 phosphorylation and increased in Kif26b abundance (Fig. 2 C and D). Thus, these results indicate that Ror receptors are required to facilitate Wnt5a-driven regulation of Pdzrn3 abundance, which is a genuine endogenous Wnt5a-Ror signaling event.

To test whether Wnt5a regulation of Pdzrn3 protein abundance also occurs transcriptionally, we treated Wnt5a KO MEFs with rWnt5a for 1 or 6 h and analyzed the levels of Pdzrn3 mRNA by reverse-transcription quantitative PCR (RT-qPCR). Unlike Pdzrn3 protein, Pdzrn3 transcripts did not change significantly after 1 or 6 h of rWnt5a stimulation (Fig. 2E). Thus, Wnt5a-Ror signaling regulates Pdzrn3 protein abundance through a posttranscriptional mechanism. Overall, these experiments establish that regulation of Pdzrn3 protein abundance is a physiological response of Wnt5a-Ror signaling.

A Noncanonical Wnt Signaling Cascade Involving Fzd, Dvl, CK1, GSK3, and the UPS Regulates Pdzrn3 Degradation.
To dissect the molecular mechanisms mediating Wnt5a regulation of Pdzrn3, we designed a flow cytometry-based reporter in which we stably expressed GFP-Pdzrn3 in NIH/3T3 cells (referred to as WRP reporter cells, for Wnt5a-Ror-Pdzrn3). Consistent with our observations in primary

www.manaraa.com
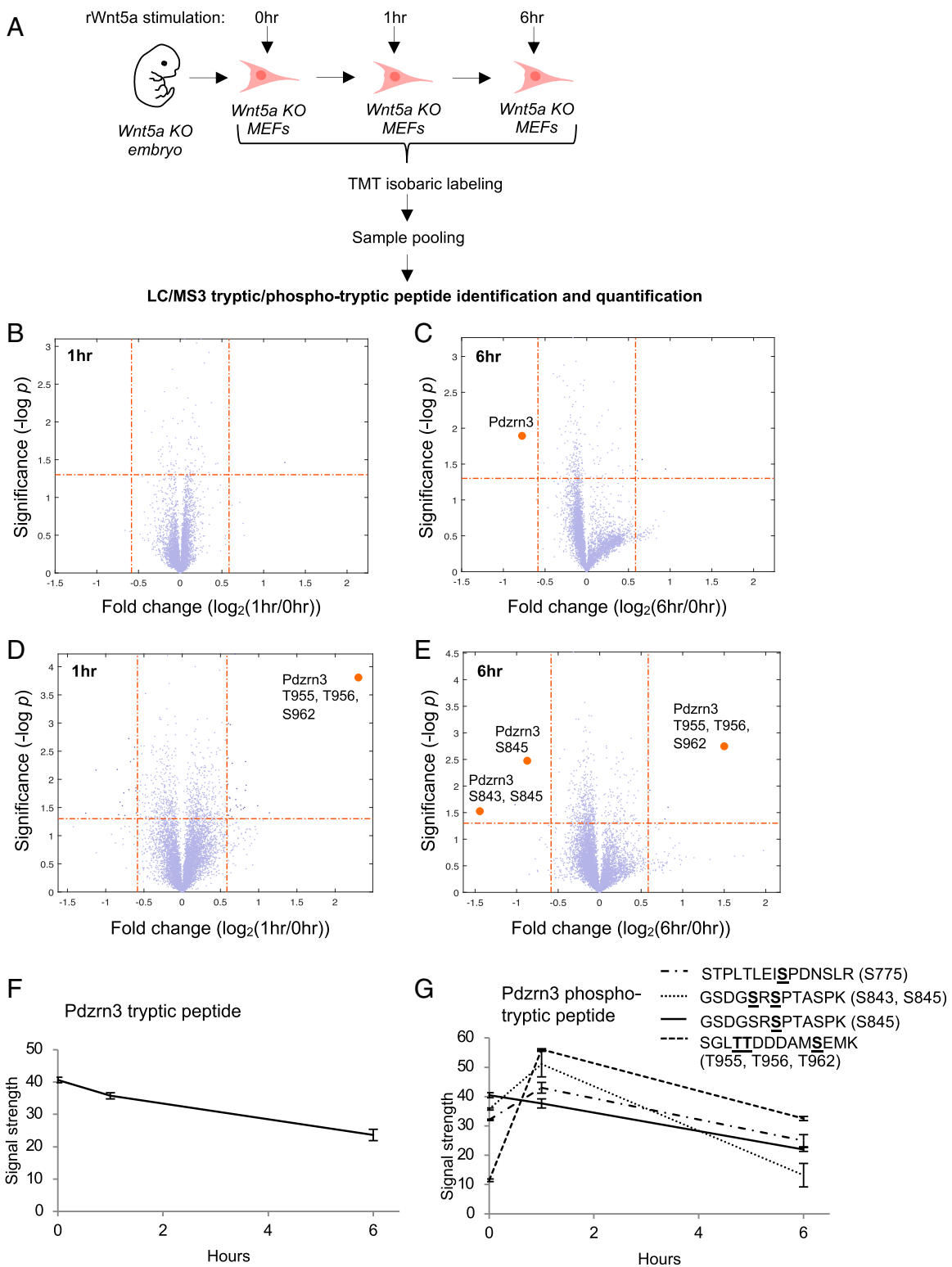
Fig. 1. Identification of the E3 ubiquitin ligase Pdzrn3 as a downstream regulatory target of Wnt5a-Ror signaling. (*A*) Workflow of whole-cell proteomics screen. Primary MEF cultures were generated from *Wnt5a* KO E12.5 mouse embryos and stimulated with rWnt5a (0.1 μg/mL) for 0, 1, or 6 h. After rWnt5a stimulation, whole-cell lysates were collected and processed for LC/MS3 tryptic/phospho-tryptic peptide identification and quantification. The rWnt5a stimulation and proteomic analysis were conducted in two independent technical replicates. (*B* and *C*) Volcano plots showing changes in the abundance of detected tryptic peptides in response to rWnt5a stimulation (0.1 μg/mL) after 1 h (*B*) or 6 h (*C*). The abundance of a tryptic peptide from Pdzrn3 (orange dots) changed strongly after 6 h of rWnt5a stimulation. (*D* and *E*) Volcano plots showing changes in the abundance of detected phospho-tryptic peptides after 1 h (*D*) or 6 h (*E*) of rWnt5a stimulation (0.1 μg/mL). Five phosphosites from Pdzrn3 (S843, S845, T955, T956, and S962) grouped in two clusters within the protein were detected and exhibited distinct patterns of change after rWnt5a stimulation (orange dots). (*F* and *G*) Line plots showing Wnt5a-induced changes in the abundance of individual tryptic (*F*) or phospho-tryptic peptides (*G*) from Pdzrn3 after 1 h or 6 h of rWnt5a stimulation. A sixth phospho-tryptic peptide site (S775) in did not pass the initial filter ($P = 0.076$), but also showed clear changes with rWnt5a stimulation. Underlined letters in (*G*) indicate phosphorylated serines or threonines within the detected peptide. Error bars represent ± SEM calculated from two technical replicates.
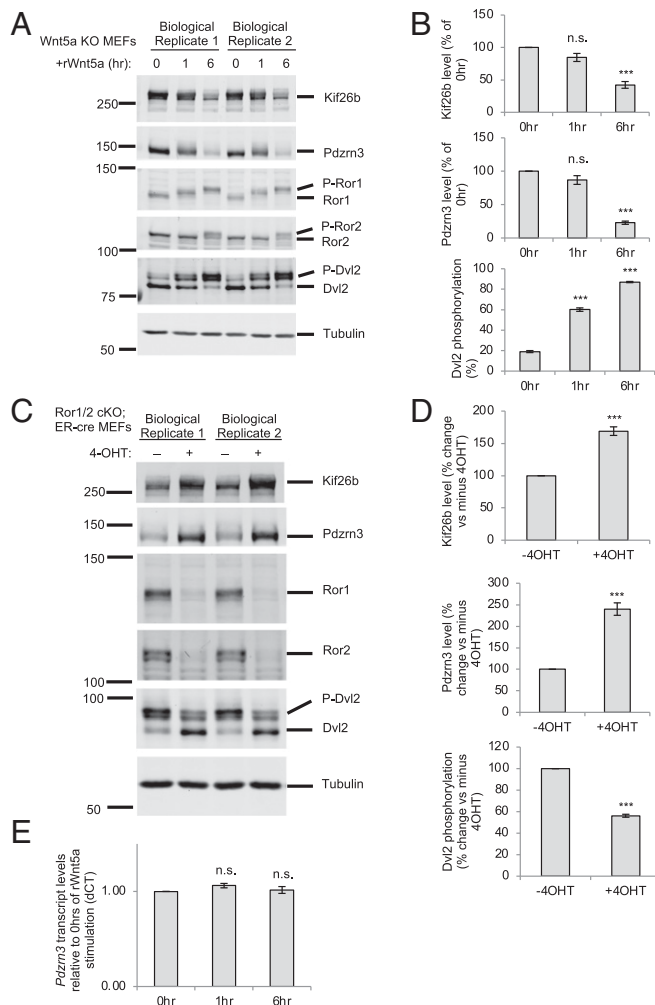
Fig. 2. Validation of Pdzrn3 as a downstream regulatory target of Wnt5a-Ror signaling. (*A*) Western blot showing down-regulation of Pdzrn3 steady-state levels in response to rWnt5a stimulation. Primary *Wnt5a* KO MEF cultures were stimulated with rWnt5a (0.2 μg/mL) for 0, 1, or 6 h, and membranes were blotted with antibodies against Kif26b, Pdzrn3, Ror1, Ror2, Dvl2, and Tubulin. P-Ror1, P-Ror2, and P-Dvl2 indicate the phoshphorylated versions of these proteins. (*B*) Quantification of *A*. (*C*) Western blots showing the requirement of endogenous Ror receptors for Pdzrn3 regulation. Protein lysates were analyzed by Western blotting using antibodies against Kif26b, Pdzrn3, Ror1, Ror2, Dvl2, and Tubulin. (*D*) Quantification of *C*. (*E*) Plot showing the effect of Wnt5a stimulation on *Pdzrn3* transcript levels. Primary *Wnt5a* KO MEFs were stimulated with rWnt5a (0.2 μg/mL) for 0, 1, or 6 h, and the relative abundance of *Pdzrn3* mRNA was determined by RT-qPCR. Error bars represent ± SEM. ***$P < 0.001$; n.s., not significant.

Wnt5a KO MEFs, treating WRP reporter cells with rWnt5a for 6 h, under conditions in which endogenous Wnt signaling was inhibited with the small-molecule PORCN inhibitor Wnt-C59, resulted in a significant down-regulation of GFP-Pdzrn3 reporter signal, thereby demonstrating the fidelity of this reporter assay (Fig. 3*A*). Moreover, we established that a saturable dose-dependent relationship exists between rWnt5a concentrations and GFP-Pdzrn3 down-regulation, with a calculated EC$_{50}$ of 77.1 ng/mL, which is similar to other Wnt-induced responses (Fig. 3*B*) (11, 43–47).

We next used WRP reporter cells to investigate the biochemical nature of Pdzrn3 down-regulation. We pharmacologically tested the role of the UPS in Pdzrn3 down-regulation as the UPS is a major regulatory pathway involved in many signaling systems and our previous study demonstrated that it is required for Wnt5a-dependent degradation of Kif26b (20). We treated WRP cells with a panel of
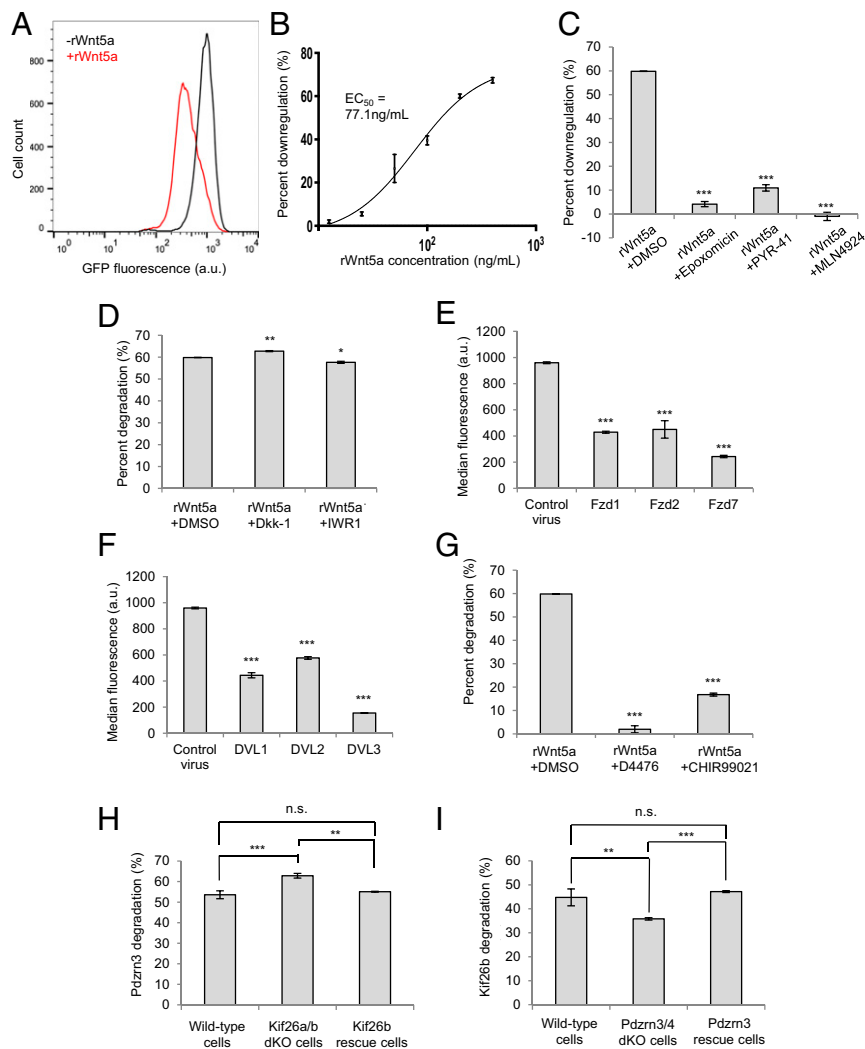
small-molecule inhibitors that block different components of the UPS: epoxomicin, which targets the proteasome (48); PYR-41, which targets the ubiquitin-activating enzyme E1 (49); and MLN4924, which targets Cullin E3 ligases (50). Each of these drugs significantly inhibited Wnt5a-dependent Pdzrn3 down-regulation (Fig. 3*C*), indicating that the UPS and the Cullin family of E3 ligases are required for Wnt5a-dependent degradation of Pdzrn3.

To test whether Wnt5a-Ror–dependent Pdzrn3 degradation occurs via noncanonical Wnt signaling mechanisms independent of the Wnt/β-catenin pathway, we treated WRP reporter cells with Dkk-1 and IWR-1-endo, which block canonical Wnt/β-catenin signaling at the receptor and destruction complex level, respectively (51–53). We observed that neither inhibitor blocked Wnt5a-induced degradation of GFP-Pdzrn3, indicating that this regulation occurs independently of the canonical Wnt pathway (Fig. 3*D*). Similarly, we observed that the prototypic canonical Wnt ligand, rWnt3a, can also drive degradation of Pdzrn3, but this regulation likely occurs through a noncanonical mechanism as it is also insensitive to Dkk1-1 and IWR-1 treatment (*SI Appendix*, Fig. S1). This finding is similar to what we previously reported for Kif26b and suggests that Wnt3a can signal noncanonically in some contexts or, alternatively, that rWnt3a can exhibit promiscuous activity within our experimental setting (20). Furthermore, we noted that both inhibitors, in the absence of either rWnt5a or rWnt3a, slightly increased the basal fluorescence of the GPF-Pdzrn3 reporter; the mechanism behind this regulation is currently unclear. Collectively, these results demonstrate that Wnt5a-Ror-Pdzrn3 signaling is a bona fide noncanonical Wnt pathway.

We next investigated if other established Wnt signaling mediators are also involved in Pdzrn3 degradation. We focused on the Fzd1, Fzd2, and Fzd7 subfamily of Fzd receptors and all three members of the family of Dvl scaffolding proteins based on their emerging connection to Robinow syndrome (12–18). We overexpressed mouse Fzd1, Fzd2, or Fzd7 and human DVL1, DVL2, or DVL3 in WRP reporter cells via lentivirus-mediated transduction and observed that overexpression of each Fzd and DVL protein mimicked the effect of rWnt5a by decreasing the WRP reporter signal significantly, whereas overexpression of the Myc eptitope tag as a negative control did not decrease WRP reporter fluorescence (Fig. 3 *E* and *F*). These findings suggest that Fzd and DVL family proteins function downstream of Wnt5a to regulate Pdzrn3 degradation.

Beyond Fzd and DVL proteins, several kinases are known to be involved in both canonical and noncanonical Wnt signaling; specifically, GSK3 and CK1 have been reported to phosphorylate Ror receptors (54, 55), and Dvl2 and Dvl3 (43, 56), respectively. To address whether these phosphorylation events are required for Wnt5a-dependent regulation of Pdzrn3, we treated WRP reporter cells with small-molecule inhibitors targeting CK1 (D4476) or GSK3 (CHIR99021). Both treatments significantly reduced Wnt5a-induced GFP-Pdzrn3 degradation (Fig. 3*G*), thus demonstrating a functional role of both CK1 and GSK3 in Wnt5a-Ror-Pdzrn3 signal transduction.

We previously reported that the atypical kinesin Kif26b is another downstream regulatory target of Wnt5a-Ror signaling (20, 57). Because Pdzrn3 and Kif26b are both regulated by the Wnt5a-Ror-Dvl axis, we sought to define the epistatic relationship between Pdzrn3 and Kif26b (i.e., whether these two proteins function in a linear cascade or in parallel branches). To distinguish between these possibilities, we used CRISPR/Cas9 gene editing to generate cells lacking Kif26b and its homolog Kif26a (Kif26a/b dKO cells) (*SI Appendix*, Fig. S2), which we previously showed is also a target of Wnt5a-Ror signaling (57), and tested whether the GFP-Pdzrn3 reporter is still degraded with rWnt5a stimulation. We observed that genetic deletion of *Kif26a* and *Kif26b* did not hinder rWnt5a-induce GFP-Pdzrn3 degadation; however, there was a slight but significant increase in GFP-Pdzrn3 degradation in the Kif26a/b dKO cells that was reversed with reexpression of

Konopelski Snavely et al.
Proteomic analysis identifies the E3 ubiquitin ligase Pdzrn3 as a regulatory target of
Wnt5a-Ror signaling

Fig. 3. A signaling cascade links noncanonical Wnt5a-Ror signaling to Pdzrn3 degradation. (*A*) Representative histogram showing the effect of rWnt5a treatment on NIH/3T3 GFP-Pdzrn3 (WRP) reporter cells. WRP cells were treated with rWnt5a (0.2 μg/mL) for 6 h, and GFP-Pdzrn3 fluorescence was measured by flow cytometry. (*B*) Dose–response curve showing GFP-Pdzrn3 down-regulation as a function of rWnt5a concentration in the WRP reporter assay. (*C*) Quantification of the effects of proteasome inhibitor (epoxomicin, 10 μM), ubiquitin-activating enzyme E1 inhibitor (PYR41, 10 μM) and Cullin inhibitor (MLN4924, 10 μM) on rWnt5a-induced Pdzrn3 down-regulation in WRP reporter cells. (*D*) Quantification of the effects of canonical Wnt inhibitors, Dkk-1 (2 μg/μL) and IWR-1-endo (10 μM) on rWnt5a-induced Pdzrn3 degradation in the WRP reporter cells. (*E*) Quantification of the effects of Fzd1, Fzd2, and Fzd7 overexpression on the median fluorescence of WRP reporter cells. (*F*) Quantification of the effects of DVL1, DVL2, and DVL3 overexpression on the median fluorescence of WRP reporter cells. (*G*) Quantification of the effects of CK1 (D4476, 100 μM) and GSK (CHIR99021, 100 μM) inhibitors on rWnt5a-induced Pdzrn3 degradation in the WRP reporter cells. (*H*) Quantification of the effect of genetically ablating *Kif26a* and *Kif26b* on rWnt5a-induced GFP-Pdzrn3 reporter degradation. (*I*) Quantification of the effect of genetically ablating *Pdzrn3* and *Lnx4* on rWnt5a-induced GFP-Kif26b reporter degradation. Error bars represent ± SEM. $*P < 0.05$, $**P < 0.01$, $***P < 0.001$. n.s., not significant.

Kif26b (Fig. 3*H*). In the converse experiment, we again used CRISPR/Cas9 to generate cells lacking *Pdzrn3* and its homolog *Lnx4* (Pdzrn3/4 dKO cells) (*SI Appendix*, Fig. S2), which is structurally similar to Pdzrn3 (see, for example, Fig. 5*A*). We observed that rWnt5a-induced GFP-Kif26b degradation still largely occurred (Fig. 3*I*). However, loss of *Pdzrn3* and *Lnx4* did slightly reduce GFP-Kif26b degradation, which was alleviated upon reexpression of Pdzrn3. Taken together, these data indicate that Wnt5a regulation of Pdzrn3 does not require Kif26b and vice versa, suggesting that these two targets are epistatically parallel to each other. However, there may be some degree of cross-talk through a currently unknown mechanism.

Pdzrn3 Phosphorylation Is Required for Its Degradation and Serves as a Molecular Switch to Modulate Wnt5a-Driven Cell Migration. We next sought to define the structural elements within Pdzrn3 required for its degradation and explore the possible role of phosphorylation in

this regulation. Pdzrn3 is a cytosolic protein that contains an N-terminal RING domain that confers its putative E3 ligase activity, two internal PDZ domains that mediate protein–protein interactions, a C-terminal LNX3 homology (LNX3H) domain with no described function, and a C-terminus PDZ domain binding motif (Fig. 4*A*) (22, 58). The six phosphorylation sites identified in our phosphoproteomic analysis cluster into two groups: group 1 phosphorylation sites (S775, S843, and S845) reside within the linker region between the second PDZ domain and the LNX3H domain, and group 2 phosphorylation sites (T955, T956, and S962) are located within the LNX3H domain itself. Interestingly, while phosphorylation of group 1 sites showed only a slight increase at 1 h and then decreased after 6 h (compare Fig. 1*F* with dot-dashed, dotted, and solid lines in Fig. 1*G*), phosphorylation of group 2 sites increased significantly after 1 h of rWnt5a stimulation, prior to Pdzrn3 degradation, and then decreased after 6 h of rWnt5a stimulation

(compare Fig. 1*F* with dashed line in Fig. 1*G*), which raised the hypothesis that phosphorylation of these sites, particularly those in group 2, may be required for Wnt5a-regulation of Pdzrn3 degradation.

To test this hypothesis, we systematically generated phospho-inhibitory mutants (T- or S-to-A substitutions) of all three sites in either group 1 or group 2 and examined rWnt5a-induced Pdzrn3 degradation. We observed that while mutation of group 1 sites had no effect on rWnt5a-induced Pdzrn3 degradation, mutation of group 2 sites strongly abolished GFP-Pdzrn3 degradation (Fig. 4*B*). To further dissect which specific sites within group 2 are required for Pdzrn3 degradation, we individually mutated each of the three sites and observed that any of the three single mutations significantly reduced rWnt5a-induced GFP-Pdzrn3 degradation (Fig. 4*C*). To further test whether phosphorylation of these three residues is sufficient to mimic Wnt5a-induced Pdzrn3 degradation, we

generated a triple phosphomimetic mutant (T or S to E) and observed that these mutations, in the absence of exogenous rWnt5a stimulation, constitutively decreased the Pdzrn3 reporter signal to a level comparable to that of WT Pdzrn3 upon rWnt5a stimulation, and no further degradation was induced by rWnt5a stimulation (Fig. 4*D*). These experiments establish that Wnt5a-dependent phosphorylation of the three group 2 sites in the LNX3H domain is both required and sufficient to drive Pdzrn3 degradation.

We next investigated the cell biological consequences of Pdzrn3 phosphorylation and degradation. Since we previously demonstrated that Wnt5a-Ror signaling can modulate cell migration through regulation of Kif26b abundance (20), we wondered if Wnt5a-Ror regulation of effector abundance might be a general paradigm through which Pdzrn3 is similarly controlled. This possibility seemed particularly salient given that others have demonstrated that Pdzrn3 can function as a promigratory factor in cell
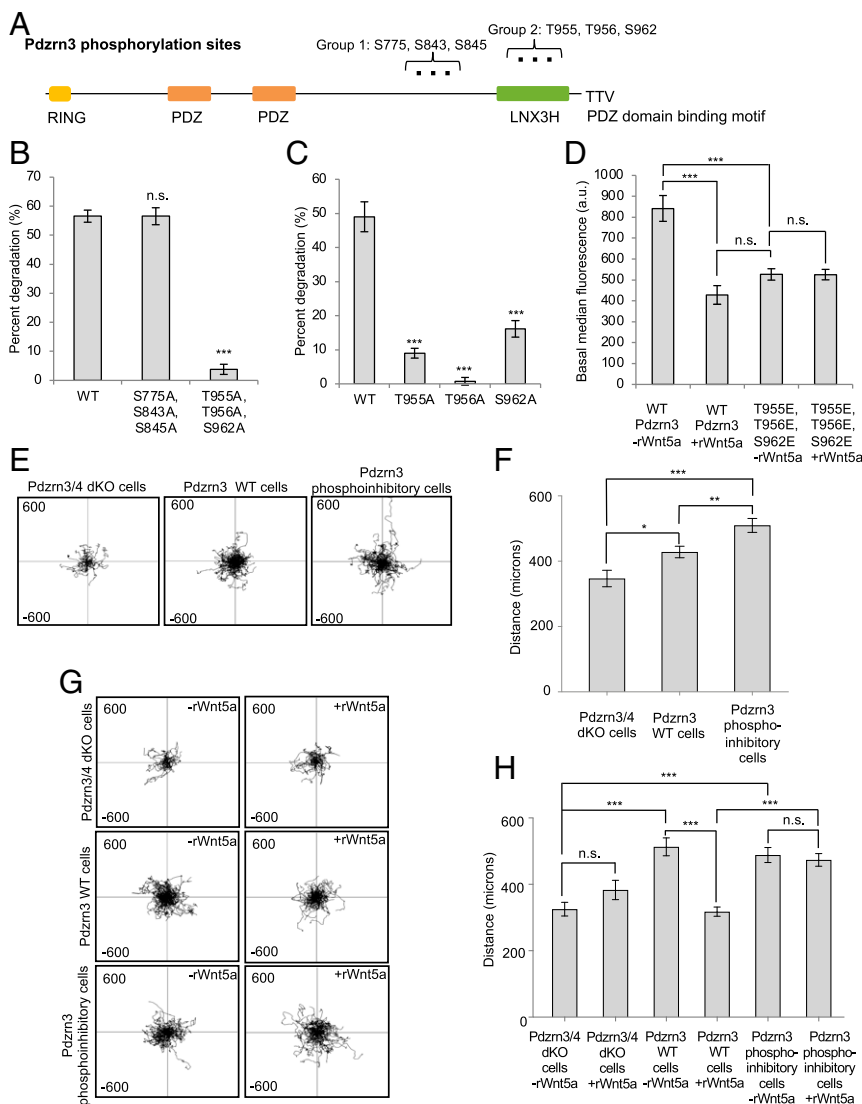
Fig. 4. Wnt5a-mediated Pdzrn3 phosphorylation is required for its degradation and modulation of cell migration. (*A*) Schematic of domains and identified phosphorylation sites of Pdzrn3. (*B*) Quantification of the effects of mutating group 1 and group 2 sites on Wnt5a-induced Pdzrn3 degradation. (*C*) Quantification of the effects of mutating individual group 2 sites on Wnt5a-induced Pdzrn3 degradation. (*D*) Quantification of the effects of group 2 phosphomimetic mutations on Pdzrn3 reporter signals. (*E*) Single-cell tracking plots of Pdzrn3 and Lnx4 dKO cells (Pdzrn3/4 dKO cells), Pdzrn3/4 dKO cells reexpressing WT Pdzrn3 (Pdzrn3 WT cells), or Pdzrn3/4 dKO cells reexpressing Pdzrn3 with phosphoinhibitory mutations at group 2 sites (Pdzrn3 phosphoinhibitory cells) without any Wnt-C59 or rWnt5a treatments. Axes extend to 600 μ. (*F*) Quantification of *E*. (*G*) Single-cell tracking plots of Pdzrn3/4 dKO cells, Pdzrn3 WT cells, and Pdzrn3 phosphoinhibitory cells treated with or without rWnt5a in the presence of Wnt-C59. Axes extend to 600 μ. (*H*) Quantification of *G*. Error bars represent ± SEM. *P < 0.05, **P < 0.01, ***P < 0.001. n.s., not significant.

www.manaraa.com

morphogenetic events (22, 23). Thus, we hypothesized that Pdzrn3 abundance might ultimately serve to regulate cell migration.

To evaluate our hypothesis, we used real-time single-cell tracking to first assess the role of Pdzrn3 itself on cell migration. We took advantage of the Pdzrn3/4 dKO cells, which provided a platform in which we could directly compare the function and regulation of WT Pdzrn3 (Pdzrn3 WT cells) to the group 2 phosphoinhibitory site mutant Pdzrn3 (Pdzrn3 phosphoinhibitory cells) without potential influence from the structural homolog Lnx4. First, we observed that cells expressing WT Pdzrn3 cells migrated significantly greater distances than Pdzrn3/4 dKO cells (Fig. 4 *E* and *F*), thereby confirming that Pdzrn3 functions as a promigratory factor (22, 23). Interestingly, we noticed that Pdzrn3 phosphoinhibitory cells migrated significantly further than both Pdzrn3/4 dKO cells and Pdzrn3 WT cells, suggesting that inhibiting Pdzrn3 phosphorylation could potentially enhance cell migration.

We next assayed for the influence of the Wnt5a-Ror-Pdzrn3 axis on cell migration. We observed that while rWnt5a stimulation had no effect on the distance traveled by Pdzrn3/4 dKO cells, it strongly reduced the distance traveled by WT Pdzrn3 cells (Fig. 4 *G* and *H*). Importantly, this Wnt5a effect on cell migration was completely abolished in Pdzrn3 phosphoinhibitory cells. Together, these results establish that phosphorylation-dependent degradation of Pdzrn3 is required for Wnt5a to modulate cell migration.

The C-Terminal LNX3H Domain Functions as a Wnt5a-Responsive Domain to Regulate Protein Abundance of Pdzrn3 and Related Homologs. Pdzrn3 belongs to the Ligand of Numb-X (Lnx) family of E3 ligases (Fig. 5*A*). Like Pdzrn3, each Lnx family member possesses an N-terminal RING domain (except Lnx5) and one to four internal PDZ binding domains. Furthermore, Lnx4 and Lnx5 each additionally possess a C-terminal LNX3H domain and a C-terminus PDZ domain binding motif (22, 58). Notably, the LNX3H domains of Lnx4 and Lnx5 also contain the group 2 phosphorylation sites found in Pdzrn3 (Fig. 5*B*). Based on our finding that these sites regulate Wnt5a-induced Pdzrn3 degradation, we hypothesized that Lnx4 and possibly Lnx5 may also be regulated by Wnt5a signals and that the LNX3H domain may function as a Wnt5a-responsive domain. To test this hypothesis, we generated reporter cell lines stably expressing GFP-Lnx1, -Lnx2, -Lnx4, or -Lnx5 fusion proteins and assessed their ability to undergo degradation in response to rWnt5a stimulation. As predicted, when stimulated with rWnt5a, GFP-Lnx1 and GFP-Lnx2 did not degrade, whereas GFP-Lnx4 exhibited a modest but significant degradation response (Fig. 5*C*). Curiously, GFP-Lnx5 did not degrade after rWnt5a stimulation (Fig. 5*C*). We therefore conclude that, like Pdzrn3, Lnx4 is also a target of Wnt5a signaling. Moreover, the Wnt5a responsiveness of Lnx family members correlates with the presence of both LNX3H and RING domains, as the primary difference between Lnx5 and Pdzrn3/Lnx4 is the N-terminal RING domain.
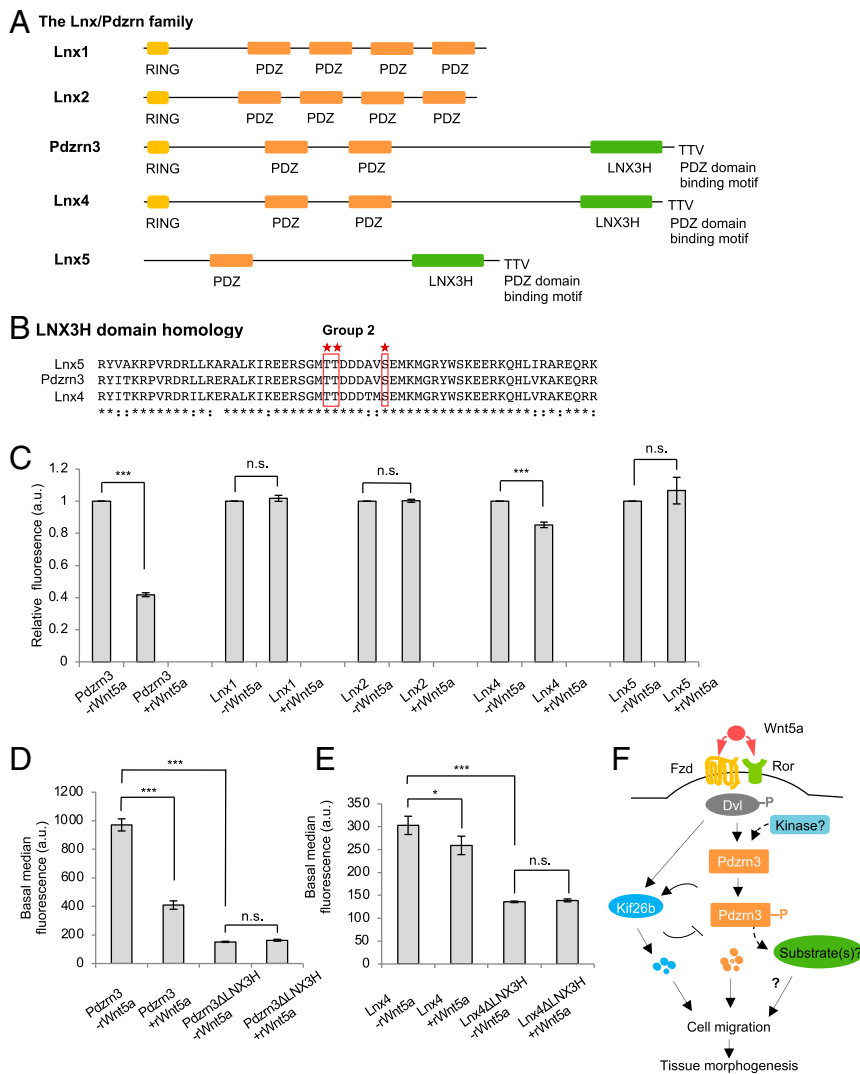
To further test the idea that the LNX3H domain might act as a Wnt5a-responsive domain, we generated truncation mutants of GFP-Pdzrn3 and GFP-Lnx4 lacking this domain. We observed that rWnt5a-induced degradation was completely abolished in these mutant cells (Fig. 5 *D* and *E*). In addition, the steady-state fluorescence of unstimulated reporter cells was also substantially reduced (Fig. 5 *D* and *E*). These observations suggest that the LNX3H domain of Pdzrn3 and Lnx4 acts not only as a Wnt5a-responsive domain but may do so by regulating overall protein stability, possibly by inhibiting the N-terminal RING domain to prevent autoubiquitination and degradation. While the mechanism by which the LNX3H domain responds to Wnt5a signals remains unknown and is beyond the scope of this study, our finding defines the LNX3H domain as a bona fide Wnt5a-responsive domain that regulates Pdzrn3 and Lnx4 stability.

Discussion

In this study, we conducted a whole proteome-scale mass spectrometry screen in primary *Wnt5a* KO MEFs to identify early and late downstream events driven by Wnt5a-Ror signaling and identified the E3 ubiquitin ligase Pdzrn3 as a regulatory target. Activation of Wnt5a-Ror signaling results in the regulation of Pdzrn3 abundance in a β-catenin–independent manner mediated by a signaling cascade involving Fzd receptors, Dvl scaffolding proteins, GSK3, and CK1 that culminates in UPS-dependent degradation of Pdzrn3. We observed that Kif26b is not required for Wnt5a-mediated Pdzrn3 degradation nor is Pdzrn3 required for Kif26b degradation, although there is some potential cross-talk between the two effectors (Fig. 5*F*). Importantly, we determined that the Wnt5a-Ror-Pdzrn3 signaling axis serves to modulate cell migration. Wnt5a-induced Pdzrn3 phosphorylation at three residues on its C-terminal LNXH3 domain is required for its subsequent degradation, which is also required for Wnt5a-Ror signaling to reduce cell migration in NIH/3T3 cells. Thus, the biochemical changes observed in our Wnt5a-Ror signaling cascade connect to a distinct cell biological behavior. Finally, we noted that truncation of the LNX3H domain results in constitutive destabilization of Pdzrn3 even in the absence of Wnt5a, suggesting that the LNX3H domain may function as both a Wnt5a-responsive domain and an intrinsic regulator of Pdzrn3 stability. From these findings, we propose that the LNX3H domain of Pdzrn3 may function to prevent Pdzrn3 autoubiquitination and self-degradation mediated by its RING domain. Prior to Wnt5a stimulation, Pdzrn3 may adopt a "closed" conformation as its C-terminal PDZ domain binding motif interacts with one of its internal PDZ domains to block its E3 ligase activity. Upon Wnt5a stimulation, Pdzrn3 is C-terminally phosphorylated on its LNX3H domain by an unidentified kinase to switch the "closed" conformation into an "open" conformation, allowing Pdzrn3 to catalyze the ubiquitination of its substrates and itself. Notably, this opened/closed conformation paradigm has been previously described in other components of Wnt signaling, including Axin and Dvl (59–61). Conceivably, the equilibrium between the closed and open Pdzrn3 could be modulated through either intramolecular interactions within a single Pdzrn3 molecule or through intermolecular interactions between Pdzrn3 dimers or multimers. Future detailed biochemical experiments are required to directly evaluate these possibilities as well as assess whether Pdzrn3 is phosphorylated by a kinase known to be involved in noncanonical Wnt signaling (e.g., CK1 or GSK3) or another one, as well as how the kinase itself is regulated by Wnt5a-Ror signaling.

It is well established that several core components of canonical Wnt signaling (e.g., β-catenin, adenomatous polyposis coli, and Axin) are regulated by proteasomal degradation (53, 62, 63). The present work, together with other recent studies, establishes that multiple effectors of noncanonical Wnt pathways—including Pdzrn3, Kif26a, Kif26b, and Syndecan4—are also subject to regulation by the ubiquitin-proteasome pathway (20, 57, 64). Collectively, these findings suggest that regulated proteolysis to tune the abundance of downstream effectors and thus, signaling outcomes, may be a conserved paradigm common to both canonical and noncanonical Wnt signaling pathways. This concept will continue to evolve as additional Wnt signaling components are characterized.

While our study addresses the biochemical regulation of Pdzrn3 by Wnt5a-Ror signaling, previous work supports the physiological importance of Pdzrn3 in noncanonical Wnt signaling. One particularly notable study focuses on the role of Pdzrn3 in vascular morphogenesis during embryonic development (22). Here, Sewduth et al. (22) identified a binding interaction between Pdzrn3 and Dvl3 via a yeast two-hybrid screen and subsequent coimmunoprecipitation, going on to demonstrate that loss of Pdzrn3 in vivo results in increased vasculature disorganization in both the embryonic yolk sac and developing mouse brain. Furthermore, deletion of Pdzrn3 reduces persistent directional migration in human umbilical vein

Konopelski Snavely et al.
Proteomic analysis identifies the E3 ubiquitin ligase Pdzrn3 as a regulatory target of Wnt5a-Ror signaling

PNAS | 7 of 10
https://doi.org/10.1073/pnas.2104944118
www.manaraa.com

Fig. 5. The C-terminal LNX3H domain acts as a general Wnt5a-responsive domain for Pdzrn3 and its homologs. (*A*) Schematic of Lnx family members and their conserved domains. Pdzrn3 is structurally most homologous to Lnx4. (*B*) Alignment of a portion of the LNX3H domain shared by Pdzrn3, Lnx4, and Lnx5. The Pdzrn3 group 2 phosphorylation sites identified through our mass spectrometry screen are conserved (red stars and boxes). (*C*) Quantification of the effects of Wnt5a on the steady-state abundance of GFP-Lnx family member reporter cell lines. For clarity and ease of comparison across family members, the median reporter signal for the +Wnt5a condition was normalized to the −Wnt5a condition within the individual Lnx reporter. (*D*) Quantification of the effect of LNX3H truncation mutation on Pdzrn3 steady-state abundance. (*E*) Quantification of the effect of LNX3H truncation mutation on Lnx4 steady-state abundance. (*F*) Model of Wnt5a-Ror-Dvl-Pdzrn3 signaling. Error bars represent ± SEM. *P < 0.05, ***P < 0.001. n.s., not significant.

endothelial cells in vitro. Importantly, our findings further build upon this model by demonstrating that Wnt5a-Ror signaling modulates cell migration through Pdzrn3 by triggering its phosphorylation and subsequent degradation. Our study, in conjunction with existing Pdzrn3 literature, indicates that changes in Pdzrn3 abundance results in noncanonical Wnt signaling defects that can be observed at the molecular, cell, and organismal levels, supporting a physiologically relevant role for Pdzrn3 in Wnt5a-dependent morphogenetic regulation.

Although the substrates ubiquitinated by Pdzrn3 (or Pdzrn3-containing E3 ligase complexes) during active Wnt5a-Ror signaling remain unclear, previous work examining the role of Pdzrn3 at the neuromuscular junction may provide a clue. Lu et al. (21) reported that PDZRN3 regulates MuSK (muscle-specific kinase) receptor expression levels at the surface of myotubes adjacent to the neuromuscular junction through ubiquitination, leading to their endocytosis from the cell surface and down-regulation of signaling. Given the high degree of homolog between MuSK and ROR1/ROR2 receptors (65–67), it is possible that Pdzrn3 may similarly

regulate Ror receptor trafficking to limit their surface availability; by inducing the degradation of Pdzrn3, Wnt5a may in turn increase Ror receptor levels on the cell surface. Alternatively, Pdzrn3 might ubiquitin-label Ror1 and Ror2 for trafficking purposes to enhance signaling. Identifying the physiologically relevant substrates of Pdzrn3 will be crucial to test this hypothesis in future studies.

The similar means by which Pdzrn3 and Kif26b are regulated indicate that the Wnt5a-Ror pathway has evolved multiple effectors to exert appropriate biological outcomes. Pdzrn3 and Kif26b are regulated by highly similar signaling cascades that utilize known Wnt signaling components, including Ror receptors, Dvl scaffolding proteins, and GSK3, culminating in UPS-dependent degradation of both effectors. Furthermore, both Pdzrn3 and Kif26b perform related functions at the cell behavioral level. Here, we describe the mechanism by which Wnt5a-Ror signaling utilizes Pdzrn3 phosphorylation and degradation to modulate NIH/3T3 cell migration. This paradigm is remarkably similar to the one we reported previously, wherein Wnt5a-mediated Kif26b degradation also results in decreases in cell migration as assayed via wound closure in scratch

assays (20). Our genetic epistasis experiments indicate that Pdzrn3 and Kif26b reside neither upstream nor downstream of each other but do influence each other's Wnt5a-driven degradation, further suggesting that these two components work in parallel to properly execute signaling functions.

However, it is curious that neither *Pdzrn3* nor *Kif26b* mutant mice exhibit the systemic tissue truncation phenotypes of *Wnt5a* and *Ror1; Ror2* double mutants. *Kif26b* mutant mice display kidney agenesis/hypoplasia and primordial germ cell migration phenotypes (20, 68), while *Pdzrn3* mutants display the vascular defects described above. These distinct tissue-specific phenotypes of *Kif26b* and *Pdzrn3* imply that multiple downstream signaling effectors likely exist to carry out the many biological functions of the pathway. Alternatively, there may be compensatory effects driven by closely related homologs (e.g., Lnx4 and Kif26a). These different phenotypic outcomes necessitate the evaluation of a *Pdzrn3; Kif26b;* double-mutant mice in addition to further identification of potential Wnt5a-Ror signaling targets.

The lack of quantitative and reliable readouts for Wnt5a-Ror signaling has been a major limitation in the field. We leveraged our discovery of Pdzrn3 and its regulation by Wnt5a-Ror signaling to develop a flow cytometry-based reporter that enables sensitive and quantitative detection of pathway activity in live cells. Beyond dissecting the mechanisms that mediate Pdzrn3 degradation, this reporter assay could also be utilized to interrogate other biochemical steps in the pathway upstream of Pdzrn3, understand various disease-associated mutations, and serve as an important platform for high-throughput screening of small molecules that target Wnt5a-Ror–driven developmental disorders and cancers.

Materials and Methods

Briefly, fully confluent primary *Wnt5a*$^{-/-}$ MEFs pooled from multiple mouse embryos were treated either with rWnt5a (100ng/mL final concentration) for 1 h or 6 h, or with the control buffer (1× PBS, 0.1% bovine serum albumin, 0.5% [wt/vol] CHAPS) for 6 h and prepared for TMT/MS3 analysis. Quantitative Western blotting was performed using the Odyssey infrared imaging system (Li-Cor Biosciences) according to the manufacturer's instructions. Quantitative flow cytometry was performed by plating and treating NIH/3T3 reporter cells with Wnt5-C59 for 48 h prior to analysis. All rWnt5a stimulations and inhibitor pretreatments and treatments were conducted in the presence of Wnt-C59 on the day of collection. Cells were analyzed using a flow cytometer (Becton Dickinson FACScan, 488-nm laser) and raw data were processed in FlowJoX (Tree Star). For two-dimensional live-cell migration experiments, resultant cells were cultured in complete media or in Wnt-C59 containing media for 72 h (for experiments involving rWnt5a stimulation) prior to plating, with rWnt5a treatment starting immediately prior to imaging. Multipoint time-lapse images were collected every 10 min for 20 h on an Andor Dragonfly spinning-disk confocal system in a humidity-controlled chamber (37 °C). Cell migration was tracked using the ImageJ manual tracking plugin, and total distance traversed was calculated using the ImageJ Chemotaxis tool plugin. Detailed methods are provided in *SI Appendix, Materials and Methods*.

Data Availability. All study data are included in the article and *SI Appendix*.

1. H. Clevers, R. Nusse, Wnt/β-catenin signaling and disease. *Cell* **149**, 1192–1205 (2012).
2. R. Nusse, H. Varmus, Three decades of Wnts: A personal perspective on how a scientific field developed. *EMBO J.* **31**, 2670–2684 (2012).
3. Z. Steinhart, S. Angers, Wnt signaling in development and tissue homeostasis. *Development* **145**, dev146589 (2018).
4. M. T. Veeman, J. D. Axelrod, R. T. Moon, A second canon. Functions and mechanisms of beta-catenin-independent Wnt signaling. *Dev. Cell* **5**, 367–377 (2003).
5. A. J. Mikels, R. Nusse, Purified Wnt5a protein activates or inhibits beta-catenin-TCF signaling depending on receptor context. *PLoS Biol.* **4**, e115 (2006).
6. I. Oishi et al., The receptor tyrosine kinase Ror2 is involved in non-canonical Wnt5a/JNK signalling pathway. *Genes Cells* **8**, 645–654 (2003).
7. R. T. Moon et al., Xwnt-5A: A maternal Wnt that affects morphogenetic movements after overexpression in embryos of Xenopus laevis. *Development* **119**, 97–111 (1993).
8. T. P. Yamaguchi, A. Bradley, A. P. McMahon, S. Jones, A Wnt5a pathway underlies outgrowth of multiple structures in the vertebrate embryo. *Development* **126**, 1211–1223 (1999).
9. H. Hikasa, M. Shibata, I. Hiratani, M. Taira, The Xenopus receptor tyrosine kinase Xror2 modulates morphogenetic movements of the axial mesoderm and neuroectoderm via Wnt signaling. *Development* **129**, 5227–5239 (2002).
10. M. Nomi et al., Loss of mRor1 enhances the heart and skeletal abnormalities in mRor2-deficient mice: Redundant and pleiotropic functions of mRor1 and mRor2 receptor tyrosine kinases. *Mol. Cell. Biol.* **21**, 8329–8335 (2001).
11. H. Y. Ho et al., Wnt5a-Ror-Dishevelled signaling constitutes a core developmental pathway that controls tissue morphogenesis. *Proc. Natl. Acad. Sci. U.S.A.* **109**, 4044–4051 (2012).
12. A. R. Afzal et al., Recessive Robinow syndrome, allelic to dominant brachydactyly type B, is caused by mutation of ROR2. *Nat. Genet.* **25**, 419–422 (2000).
13. A. R. Afzal, S. Jeffery, One gene, two phenotypes: ROR2 mutations in autosomal recessive Robinow syndrome and autosomal dominant brachydactyly type B. *Hum. Mutat.* **22**, 1–11 (2003).
14. A. D. Person et al., WNT5A mutations in patients with autosomal dominant Robinow syndrome. *Dev. Dyn.* **239**, 327–337 (2010).
15. K. J. Bunn et al., Mutations in DVL1 cause an osteosclerotic form of Robinow syndrome. *Am. J. Hum. Genet.* **96**, 623–630 (2015).
16. J. White et al.; Baylor-Hopkins Center for Mendelian Genomics, DVL1 frameshift mutations clustering in the penultimate exon cause autosomal-dominant Robinow syndrome. *Am. J. Hum. Genet.* **96**, 612–622 (2015).
17. J. J. White et al.; Baylor-Hopkins Center for Mendelian Genomics, DVL3 alleles resulting in a -1 frameshift of the last exon mediate autosomal-dominant Robinow syndrome. *Am. J. Hum. Genet.* **98**, 553–561 (2016).
18. J. J. White et al.; Baylor-Hopkins Center for Mendelian Genomics, WNT signaling perturbations underlie the genetic heterogeneity of Robinow syndrome. *Am. J. Hum. Genet.* **102**, 27–43 (2018).
19. T. A. Mansour et al., Whole genome variant association across 100 dogs identifies a frame shift mutation in DISHEVELLED 2 which contributes to Robinow-like syndrome in Bulldogs and related screw tail dog breeds. *PLoS Genet.* **14**, e1007850 (2018).
20. M. W. Susman et al., Kinesin superfamily protein Kif26b links Wnt5a-Ror signaling to the control of cell and tissue behaviors in vertebrates. *eLife* **6**, e26509 (2017).
21. Z. Lu et al., Regulation of synaptic growth and maturation by a synapse-associated E3 ubiquitin ligase at the neuromuscular junction. *J. Cell Biol.* **177**, 1077–1089 (2007).
22. R. N. Sewduth et al., The ubiquitin ligase PDZRN3 is required for vascular morphogenesis through Wnt/planar cell polarity signalling. *Nat. Commun.* **5**, 4832 (2014).
23. J. M. Baizabal et al., The epigenetic state of PRDM16-regulated enhancers in radial glia controls cortical neuron position. *Neuron* **99**, 239–241 (2018).
24. L. Ting, R. Rad, S. P. Gygi, W. Haas, MS3 eliminates ratio distortion in isobaric multiplexed quantitative proteomics. *Nat. Methods* **8**, 937–940 (2011).
25. A. Higashimori et al., Forkhead box F2 suppresses gastric cancer through a novel FOXF2-IRF2BPL-β-catenin signaling axis. *Cancer Res.* **78**, 1643–1656 (2018).
26. M. E. O'Connell et al., The *Drosophila* protein, Nausicaa, regulates lamellipodial actin dynamics in a Cortactin-dependent manner. *Biol. Open* **8**, bio038232 (2019).
27. J. B. Zuchero, A. S. Coutts, M. E. Quinlan, N. B. Thangue, R. D. Mullins, p53-cofactor JMY is a multifunctional actin nucleation factor. *Nat. Cell Biol.* **11**, 451–459 (2009).
28. K. H. Wrighton, JMY: Actin up in cell motility. *Nat. Rev. Mol. Cell Biol.* **10**, 304 (2009).
29. M. M. Azevedo et al., Jmy regulates oligodendrocyte differentiation via modulation of actin cytoskeleton dynamics. *Glia* **66**, 1826–1844 (2018).
30. I. Tan, J. Lai, J. Yong, S. F. Li, T. Leung, Chelerythrine perturbs lamellar actomyosin filaments by selective inhibition of myotonic dystrophy kinase-related Cdc42-binding kinase. *FEBS Lett.* **585**, 1260–1268 (2011).
31. X. Chen et al., Supervillin promotes epithelial-mesenchymal transition and metastasis of hepatocellular carcinoma in hypoxia via activation of the RhoA/ROCK-ERK/p38 pathway. *J. Exp. Clin. Cancer Res.* **37**, 128 (2018).
32. J. L. Crowley, T. C. Smith, Z. Fang, N. Takizawa, E. J. Luna, Supervillin reorganizes the actin cytoskeleton and increases invadopodial efficiency. *Mol. Biol. Cell* **20**, 948–962 (2009).
33. C. Serra-Pagès, Q. G. Medley, M. Tang, A. Hart, M. Streuli, Liprins, a family of LAR transmembrane protein-tyrosine phosphatase-interacting proteins. *J. Biol. Chem.* **273**, 15611–15620 (1998).
34. B. Björkblom et al., c-Jun N-terminal kinase phosphorylation of MARCKSL1 determines actin stability and migration in neurons and in cancer cells. *Mol. Cell. Biol.* **32**, 3513–3526 (2012).
35. A. Aderem, Signal transduction and the actin cytoskeleton: The roles of MARCKS and profilin. *Trends Biochem. Sci.* **17**, 438–443 (1992).
36. T. Mayanagi, K. Sobue, Diversification of caldesmon-linked actin cytoskeleton in cell motility. *Cell Adhes. Migr.* **5**, 150–159 (2011).
37. J. J. Lin, Y. Li, R. D. Eppinga, Q. Wang, J. P. Jin, Chapter 1: Roles of caldesmon in cell motility and actin cytoskeleton remodeling. *Int. Rev. Cell Mol. Biol.* **274**, 1–68 (2009).

Konopelski Snavely et al.
Proteomic analysis identifies the E3 ubiquitin ligase Pdzrn3 as a regulatory target of Wnt5a-Ror signaling

www.manaraa.com

38. H. C. Tseng et al., Cytoskeleton network and cellular migration modulated by nuclear-localized receptor tyrosine kinase ROR1. *Anticancer Res.* **31**, 4239–4249 (2011).

39. R. Mohan, A. John, Microtubule-associated proteins as direct crosslinkers of actin filaments and microtubules. *IUBMB Life* **67**, 395–403 (2015).

40. C. Sánchez, J. Díaz-Nido, J. Avila, Phosphorylation of microtubule-associated protein 2 (MAP2) and its relevance for the regulation of the neuronal cytoskeleton function. *Prog. Neurobiol.* **61**, 133–168 (2000).

41. F. Hannes et al., A microdeletion proximal of the critical deletion region is associated with mild Wolf-Hirschhorn syndrome. *Am. J. Med. Genet. A.* **158A**, 996–1004 (2012).

42. K. M. Huang et al., Xcat, a novel mouse model for Nance-Horan syndrome inhibits expression of the cytoplasmic-targeted Nhs1 isoform. *Hum. Mol. Genet.* **15**, 319–327 (2006).

43. V. Bryja, G. Schulte, N. Rawal, A. Grahn, E. Arenas, Wnt-5a induces Dishevelled phosphorylation and dopaminergic differentiation via a CK1-dependent mechanism. *J. Cell Sci.* **120**, 586–595 (2007).

44. E. S. Witze, E. S. Litman, G. M. Argast, R. T. Moon, N. G. Ahn, Wnt5a control of cell polarity and directional movement by polarized redistribution of adhesion receptors. *Science* **320**, 365–369 (2008).

45. E. S. Witze et al., Wnt5a directs polarized calcium gradients by recruiting cortical endoplasmic reticulum to the cell trailing edge. *Dev. Cell* **26**, 645–657 (2013).

46. H. W. Park et al., Alternative Wnt signaling activates YAP/TAZ. *Cell* **162**, 780–794 (2015).

47. M. K. Connacher, J. W. Tay, N. G. Ahn, Rear-polarized Wnt5a-receptor-actin-myosin-polarity (WRAMP) structures promote the speed and persistence of directional cell migration. *Mol. Biol. Cell* **28**, 1924–1936 (2017).

48. L. Meng et al., Epoxomicin, a potent and selective proteasome inhibitor, exhibits in vivo antiinflammatory activity. *Proc. Natl. Acad. Sci. U.S.A.* **96**, 10403–10408 (1999).

49. Y. Yang et al., Inhibitors of ubiquitin-activating enzyme (E1), a new class of potential cancer therapeutics. *Cancer Res.* **67**, 9472–9481 (2007).

50. S. Tong et al., MLN4924 (Pevonedistat), a protein neddylation inhibitor, suppresses proliferation and migration of human clear cell renal cell carcinoma. *Sci. Rep.* **7**, 5599 (2017).

51. A. Bafico, G. Liu, A. Yaniv, A. Gazit, S. A. Aaronson, Novel mechanism of Wnt signalling inhibition mediated by Dickkopf-1 interaction with LRP6/Arrow. *Nat. Cell Biol.* **3**, 683–686 (2001).

52. E. Lee, A. Salic, R. Krüger, R. Heinrich, M. W. Kirschner, The roles of APC and Axin derived from experimental and theoretical analysis of the Wnt pathway. *PLoS Biol.* **1**, E10 (2003).

53. S. M. Huang et al., Tankyrase inhibition stabilizes axin and antagonizes Wnt signalling. *Nature* **461**, 614–620 (2009).

54. H. Yamamoto, S. K. Yoo, M. Nishita, A. Kikuchi, Y. Minami, Wnt5a modulates glycogen synthase kinase 3 to induce phosphorylation of receptor tyrosine kinase Ror2. *Genes Cells* **12**, 1215–1223 (2007).

55. L. Grumolato et al., Canonical and noncanonical Wnts use a common mechanism to activate completely unrelated coreceptors. *Genes Dev.* **24**, 2517–2530 (2010).

56. V. Bryja, G. Schulte, E. Arenas, Wnt-3a utilizes a novel low dose and rapid pathway that does not require casein kinase 1-mediated phosphorylation of Dvl to activate beta-catenin. *Cell. Signal.* **19**, 610–616 (2007).

57. E. P. Karuna, M. W. Susman, H. H. Ho, Quantitative live-cell reporter assay for non-canonical Wnt activity. *Bio Protoc.* **8**, e2762 (2018).

58. M. Flynn, O. Saha, P. Young, Molecular evolution of the LNX gene family. *BMC Evol. Biol.* **11**, 235 (2011).

59. S. E. Kim et al., Wnt stabilization of β-catenin reveals principles for morphogen receptor-scaffold assemblies. *Science* **340**, 867–870 (2013).

60. H. J. Lee, D. L. Shi, J. J. Zheng, Conformational change of Dishevelled plays a key regulatory role in the Wnt signaling pathways. *eLife* **4**, e08142 (2015).

61. J. Qi et al., Autoinhibition of Dishevelled protein regulated by its extreme C terminus plays a distinct role in Wnt/β-catenin and Wnt/planar cell polarity (PCP) signaling pathways. *J. Biol. Chem.* **292**, 5898–5908 (2017).

62. J. Papkoff, B. Rubinfeld, B. Schryver, P. Polakis, Wnt-1 regulates free pools of catenins and stabilizes APC-catenin complexes. *Mol. Cell. Biol.* **16**, 2128–2134 (1996).

63. J. Choi, S. Y. Park, F. Costantini, E. H. Jho, C. K. Joo, Adenomatous polyposis coli is down-regulated by the ubiquitin-proteasome pathway in a process facilitated by Axin. *J. Biol. Chem.* **279**, 49188–49198 (2004).

64. L. Carvallo et al., Non-canonical Wnt signaling induces ubiquitination and degradation of Syndecan4. *J. Biol. Chem.* **285**, 29546–29555 (2010).

65. D. J. Glass et al., The receptor tyrosine kinase MuSK is required for neuromuscular junction formation and is a functional receptor for agrin. *Cold Spring Harb. Symp. Quant. Biol.* **61**, 435–444 (1996).

66. P. Masiakowski, R. D. Carroll, A novel family of cell surface receptors with tyrosine kinase-like domain. *J. Biol. Chem.* **267**, 26181–26190 (1992).

67. D. M. Valenzuela et al., Receptor tyrosine kinase specific for the skeletal muscle lineage: Expression in embryonic muscle, at the neuromuscular junction, and after injury. *Neuron* **15**, 573–584 (1995).

68. Y. Uchiyama et al., Kif26b, a kinesin family gene, regulates adhesion of the embryonic kidney mesenchyme. *Proc. Natl. Acad. Sci. U.S.A.* **107**, 9240–9245 (2010).

Konopelski Snavely et al.
Proteomic analysis identifies the E3 ubiquitin ligase Pdzrn3 as a regulatory target of